Ion-solvating membranes as a new approach towards high rate alkaline electrolyzers

Mikkel R. Kraglund[a], Marcelo Carmo[b], Günter Schiller[c], Syed Asif Ansar[c], David Aili[a], Erik Christensen[a], Jens Oluf Jensen[a].

[a] Department of Energy Conversion and Storage, Technical University of Denmark, Elektrovej 375, DK-2800 Kgs. Lyngby, Denmark

[b] Forschungszentrum Jülich GmbH, Institute of Energy and Climate Research, IEK-3: Electrochemical Process Engineering, 52425 Jülich, Germany

[c] German Aerospace Center (DLR), Institute of Engineering Thermodynamics, 70569, Stuttgart, Germany

---

Abstract

Energy efficient and cost efficient water electrolysis is essential for the large scale implementation of renewable energy. The two commercial low temperature electrolyzer technologies each suffer from serious drawbacks. The proton exchange membrane (PEM) electrolyzers remain expensive and depend strongly on the scarce metal iridium. The alkaline electrolyzers suffer from a large footprint due to low rate capability. Here, we present an approach to make an alkaline electrolyzer perform like a PEM electrolyzer by means of an ion-solvating membrane. A long lasting effort to replace the state-of-the-art thick porous diaphragm by an anion exchange membrane has not proven successful. The ion-solvating membrane represents a third way. Demonstration cells based on KOH doped polybenzimidazole membranes and nickel based electrodes exhibited 1700 mA cm^{-2} at 1.8 V. This is far exceeding what has previously been achieved with membranes in alkaline environments without platinum group metal catalysts, and is comparable to state-of-the-art PEM electrolyzers.

The generation of hydrogen via water electrolysis is currently recognized as the only viable option to store multi gigawatt-levels of electrical energy from intermittent renewable energy sources such as wind and solar, and is essential for the decarbonisation of the transportation and industrial sectors[1]. Consequently, water electrolyzers will become increasingly important to the energy matrix, as they serve as a bridging technology between intermittent renewable electrical energy and chemical energy dependent sectors such as transportation and heavy industry.

Traditional electrolyzers based on alkaline electrolytes and porous diaphragms suffer from poor voltage efficiency, particularly at high current densities due to high internal resistance. Additionally, gas permeation through the porous diaphragms or even electrolyte blow-out is a concern. Such conventional systems are incapable of working with differential pressure and show slow response times in order to maintain balanced pressure. The overall system constraints result in a limited current density range (200-400 mA cm^{-2}) and, consequently, the hydrogen production rate is low[2,3]. On the other hand, proton exchange membrane (PEM) systems based on perfluorosulfonic acid (PFSA) membranes feature promising advantages due to their higher efficiency and wider current density window (~500-2000 mA cm^{-2}). However, PEM electrolyzers remain expensive due to their use of expensive PFSA membranes and precious platinum group metal (PGM) catalysts, *i.e.* platinum for the cathode and iridium for the anode, as well as precious metal coated titanium based components for porous transport layers and bipolar plates[3,4]. Additionally, large scale implementation will only be possible to the limit given by the availability of iridium, as it is much more scarce than platinum. There is currently no flexibility when it comes to material choices, and the channel forming nature of the PFSA membranes ultimately shows mediocre hydrogen barrier properties under pressurized operation due to diffusion, which further complicates the balance of plant and increases system costs[4].

An alkaline environment, on the other hand, allows for a cell construction completely free of PGMs and titanium based components. This has prompted substantial research on alkaline membranes for water electrolysis. A good OH^--conducting membrane could bridge the two technologies by enabling a wide range of active, non-precious metal catalysts, in combination with the low ohmic resistances and gas separation properties of a solid polymer electrolyte. The realization of alkaline membranes with sufficient conductivity and satisfactory stability could potentially induce a technological paradigm shift in which, over time, conventional alkaline systems and PEM electrolyzers get superseded.

In the quest towards improving the rate capability of alkaline electrolyzers while maintaining a reasonable degree of efficiency, significant focus has been directed towards reducing ohmic losses by developing more advanced separators and electrolyte concepts. The classical approach revolved around improving porous diaphragms[5], whereas the more recent focus has been on developing anion exchange membranes (AEMs)[6]. These two concepts are conceptually different and schematically illustrated in Figure 1a and b, respectively.

The diaphragms (Fig. 1a) are separator materials that rely solely on the liquid phase of the electrolyte to establish percolating pathways throughout the porous structure. The diaphragm matrix is made from a stable inert polymer, and is often supported by a hydrophilic inorganic filler. Previously, asbestos cloth was used, but the current commercial state-of-the-art diaphragm is made from polysulfone-bonded ZrO_2 and is often referred to by the trademark name Zirfon[7,8].

AEMs (Fig. 1b), on the other hand, have been investigated for fuel cell applications since early 2000[9], but have yet to achieve success in water electrolysis due to insufficient conductivity and stability. Such membranes are based on polymers with fixed cationic side groups paired with anions that become mobile upon dissociation in the presence of water. In that sense, AEMs are analogous to PFSA membranes, and an effective and stable ionomer phase is required in the electrode to establish a vast triple phase boundary and to conduct ions inside the catalyst layer.

We present a third alternative approach, which is based on ion-solvating membranes and a supporting electrolyte. Ion-solvating membranes, conceptually sketched in Fig. 1c, are polymeric membranes, which when imbibed with KOH swell and form a homogeneous ternary electrolyte system of polymer/water/KOH. Ion-solvating membranes utilize the uptake and presence of an aqueous alkaline electrolyte to achieve ionic conductivity, and are not necessarily intrinsic hydroxide conductors, but unlike diaphragms they are dense (non-porous) and can be prepared as thin as other polymeric membranes.

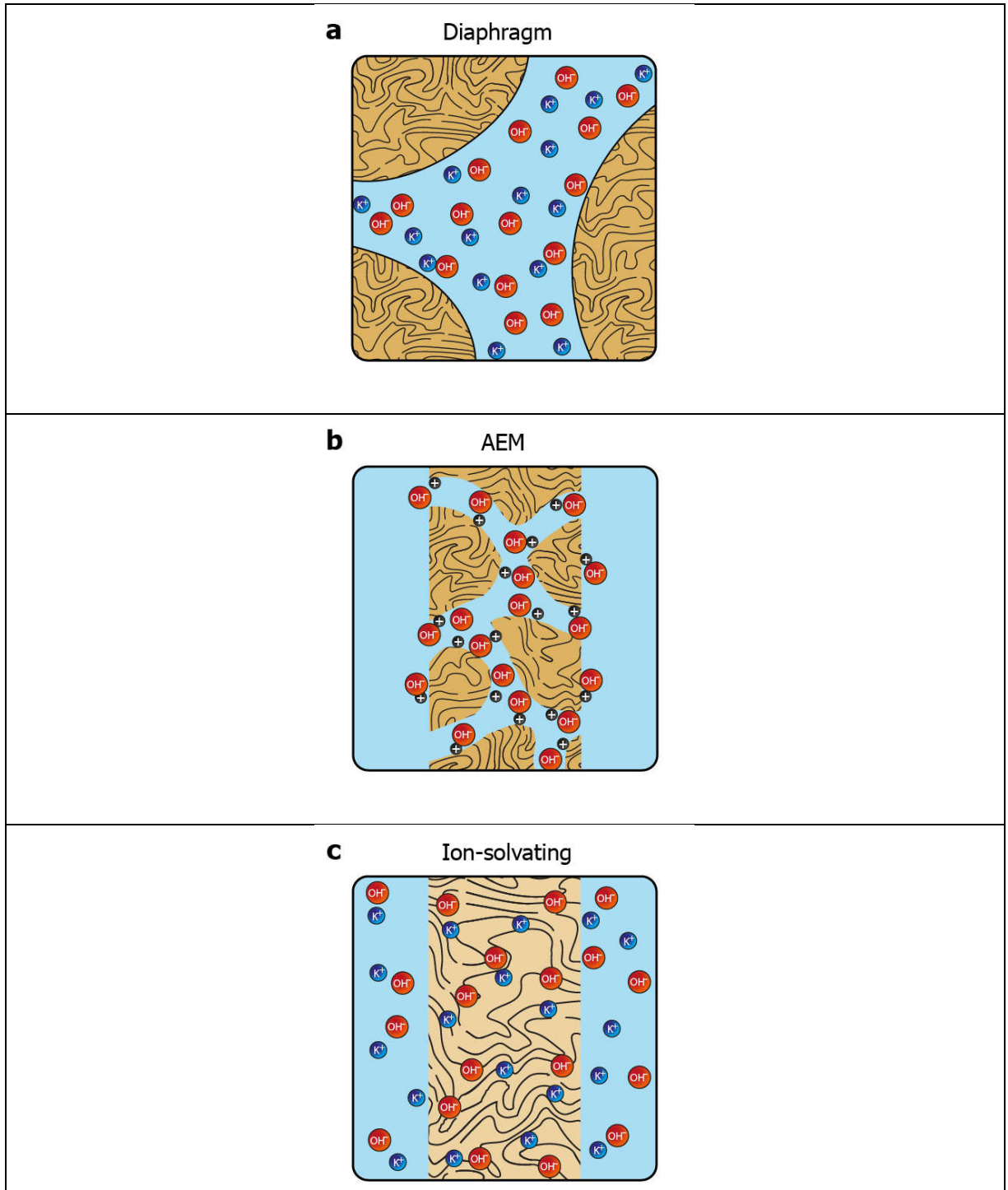

Fig. 1: Three approaches towards hydroxide conducting separators. (a) Classical diaphragm consisting of a macroporous inactive material. The pores must form a percolating network. (b) Anion exchange membrane, where positive functional groups on pendant side chains mediate

hydroxide conductivity, possibly by reorienting to form ionic channels. No aqueous electrolyte is required. (c) Ion-solvating membrane, which is imbibed with an alkaline electrolyte, commonly KOH. Significant swelling results in a homogeneous mixed phase of the polymer matrix and the electrolyte.

A key feature when using ion-solvating membranes is the supporting electrolyte. The electrolyte not only has profound effects on the membrane itself, it also affects all aspects of the electrolyzer cell, from the catalyst layers and electrodes to the balance of plant. For alkaline water electrolysis, a hydroxide electrolyte is of particular interest and hereinafter a supporting electrolyte refers to a hydroxide-based electrolyte. Screening the literature, it is evident that AEM-based cells operated with supporting electrolytes show significantly better performance than those without. This is in particular clear evident from the literature broadly, and it is in particular clear from publications that evaluate cell performance with pure water or carbonate feed, and with supporting hydroxide electrolyte feed[10–14]. An overview of published cell performance is presented in Fig. 2, with specific details available in the supplementary information. The data is grouped by the electrolyte concentration; here delimited as concentrations of KOH or NaOH above or below 0.5 M (~0.1 S cm^{-1} at room temperature), and by the presence or absence of PGM catalysts. Commonly, the used electrolyte concentrations are either equal or less than 1 wt% or at 1 M or above. On this basis, the question arises: if a supporting electrolyte is a requirement or otherwise desired for competitive cell performance, are there new avenues available to pursue instead of the conventional, functionalized pendant side-chain approach, which so far remains largely unsuccessful?

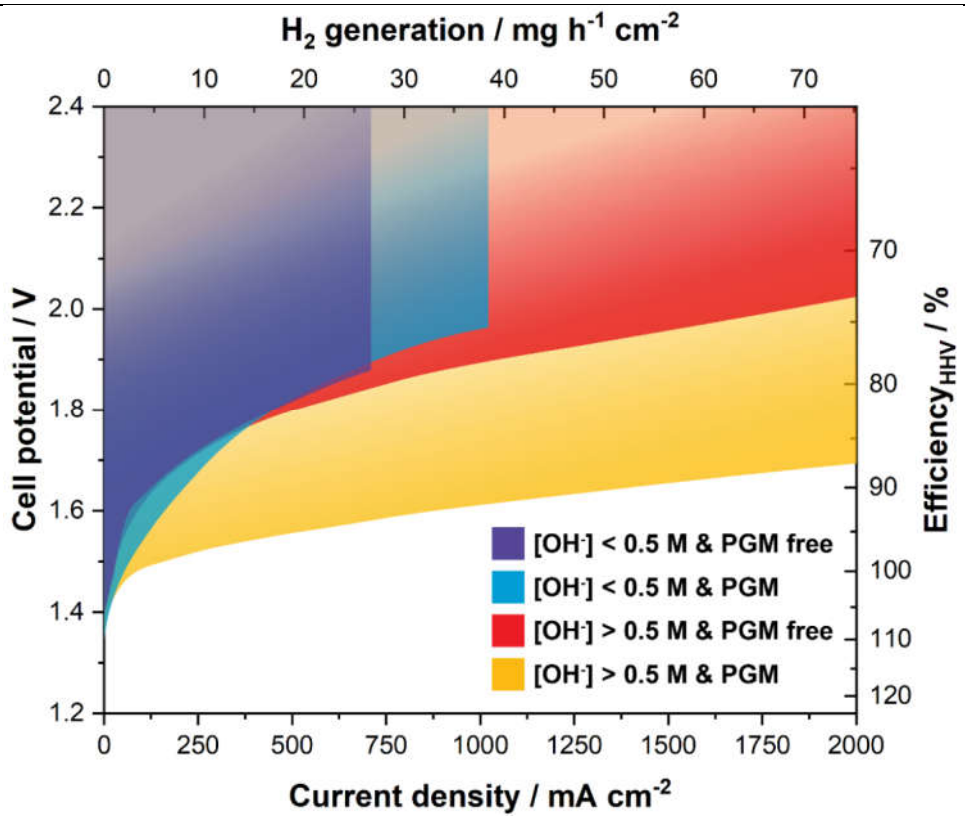

Fig. 2: Published literature performance for alkaline electrolyzer cells using polymeric membranes. The presence of a supporting electrolyte ([OH^-] > 0.5 M) improves performance and operating range. PGM catalysts still generally outperform the alternatives. The temperature range of the underlying datasets is from 22 to 80°C. References used; without supporting electrolyte and PGM free (purple)[12,39–44], without supporting electrolyte and with PGM (blue)[10,11,13,14,45–47], with supporting electrolyte and PGM free (red)[12,19,28,44,48-53] and with supporting electrolyte and with PGM (yellow)[10,11,13,14,28,54]. Further details on specific datasets are available in the supplementary information.

To demonstrate the perspectives of ion-solvating membranes, we have utilized KOH (aq)-doped poly(2,2'-(*m*-phenylene)-5,5'-bibenzimidazole) (*m*-PBI) as membrane. The KOH/mPBI system was first described by Xing and Savadogo[15] in 2000 for fuel cell applications, and we conducted the first demonstration for water electrolysis in 2013[16]. The membranes achieve the highest specific conductivity when equilibrated in bulk electrolyte concentrations in the range of 20-25 wt% KOH[17] and exhibit remarkable, though not complete stability, for up to six months in concentrated KOH[18]. They do, however, in contrast to AEMs,

show negligible conductivity in KOH concentrations below 5 wt%. To complement the membranes, we employed Raney-type nickel electrodes, which have large, electrochemically-active surface areas accessible through the supporting KOH (aq) electrolyte. For the hydrogen evolution reaction (HER), a Raney-type nickel-molybdenum cathode was used, whereas for the oxygen evolution, a Raney-type nickel anode was applied. The polarization characteristics of this cell is shown in Fig. 3, along with reference cells using state-of-the-art diaphragms and plain nickel electrodes and variations thereof. Although the cells with Raney-type electrodes and *m*-PBI membranes display an impressive rate capability of approximately 1700 mA cm^{-2} at 1.8 V and 2800 mA cm^{-2} at less than 2 V, a notable degradation in the cell potential and eventual cell failure was observed during long-term tests. While the cell voltage increase was largely due to electrode degradation, the end of life (EoL) was caused by mechanical failure of the membrane. Either in the form of electrode short circuiting, or by rapidly rising H_2 in O_2 levels on the anode side. . The two cells using 40 µm membranes showed an EoL after approximately 120 and 147 h, while cells with 89 µm membranes displayed roughly double the lifetime of 230 and 309 h respectively. Visual inspection upon cell disassembly revealed the appearance of holes or tears in the membranes (Fig. S5, ESI), as well as some loss of particulate matter from the electrodes evident in the membrane and in the KOH vessels. It has previously been shown that *m*-PBI and other polybenzimidazole derivatives experience polymer chain scission in hot and concentrated alkaline conditions,[18-21] which over time lead to mechanical failure. The process is likely accelerated under polarizing conditions due to changes in the local environment of the membrane and near the electrodes.

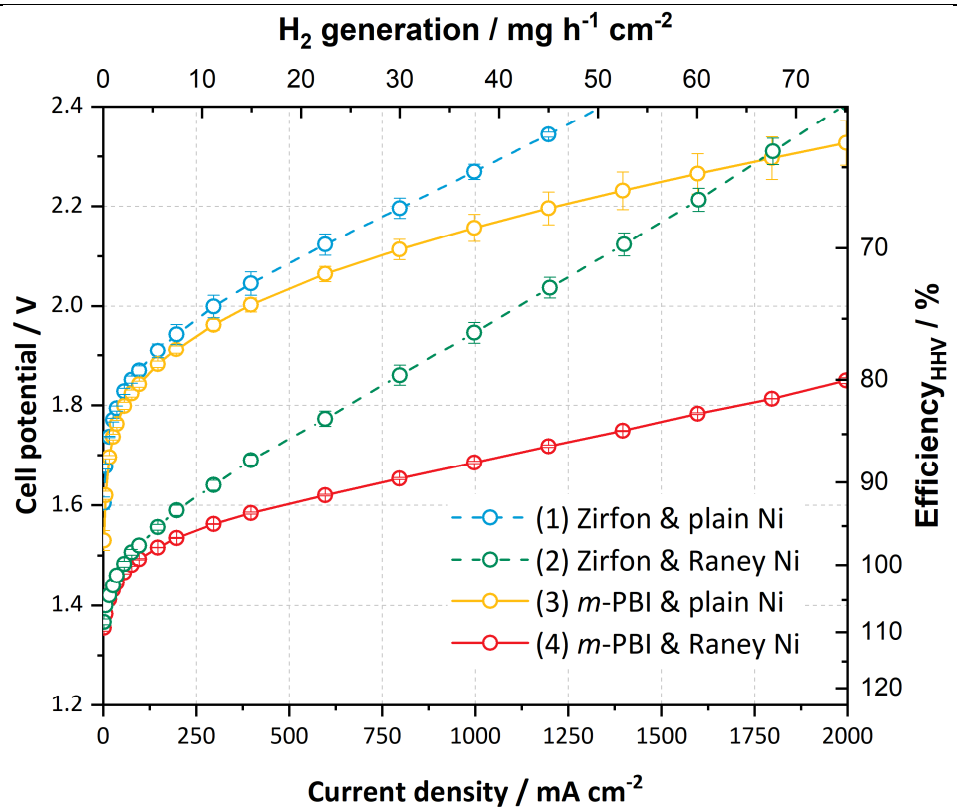

Fig. 3: Electrochemical cell performance in 24 wt% KOH and 80°C. (a) Cell polarization for four different cell configurations. Error bars represent variation between two or three cells. Cells are (cathode/separator/anode): (1) Ni-foam/Zirfon™ PERL diaphragm/Ni-perforated plate; (2) Raney-type-NiMo/Zirfon™ PERL diaphragm/Raney-type-Ni; (3) Ni-foam/40 µm *m*-PBI membrane/Ni-perforated plate; and (4) Raney-type-NiMo/40 µm *m*-PBI membrane/Raney-type-Ni.

In contrast to the membranes, Raney-type electrodes prepared by vacuum plasma spraying (VPS) have previously shown stability of more than 10 000 h.[22] However, the coatings are sensitive to the detailed preparation specifics and it is possible that the more encapsulated environment when pressed against the dense membranes result in a larger degree of pressure build-up in the pores of the coating leading to increased spallation and catalyst loss, in particular at the high current densities reached during the recording of polarization curves. Furthermore, anodic oxidation and hydroxide-oxyhydroxide formation of the nickel catalyst at the anode lead

to structural expansion and possibly a pore collapse and corresponding loss of surface area, which is supported by BET data (Table S%, ESI). Despite this and the all in all inadequate membrane stability, good performance is nonetheless achieved after a 12 h break-in as illustrated in Fig. 3, and the cells demonstrate what can be achieved using suitable electrodes and ion-solvating membranes.

One benefit of working with a supporting electrolyte is the option to omit the ionomer in the electrodes, since the aqueous electrolyte provides the necessary ionic pathways. This enables a wide range of electrode concepts to be employed, such as coated nickel foams, often labelled 3D electrodes or, as in this study, Raney-type nickel electrodes. The Raney-type nickel electrodes utilized in this work were not based on recent developments, but are well-proven and described in the literature[22-24]. Prior to cell assembly, the electrodes were activated by alkaline leaching to remove the majority of their aluminium, resulting in a highly porous material with a very large, accessible internal surface area. Additional electrode details are available in the ESI (Fig. S6 and Table S5). The pores are accessible to the aqueous electrolyte, but are unlikely to display the same activity if an ionomer is required, as effective pore infiltration without blocking is challenging. Hence these electrodes are best suited for conventional alkaline electrolysis or in membrane-based alkaline concepts including a supporting electrolyte. Although the cell system resembles classical alkaline electrolysis, the dense polymeric membrane can be effectively prepared much thinner than conventional diaphragms, and can correspondingly display much lower ohmic resistance. As we have demonstrated, a lower ohmic resistance enables the cells to operate at higher current densities, approaching or matching those of PEM electrolyzers. Using electrochemical impedance spectroscopy (EIS), the series resistance of cells using Zirfon was measured in the range of 0.24-0.30 Ω cm^2, whereas cells with 40-80 µm thick *m*-PBI membranes had values of 0.04-0.08 Ω cm^2 (Fig. S7, ESI). For comparison, the reported series resistance of PEM electrolyzer cells using Nafion 115 (127 µm) as a membrane is 0.10-0.13 Ω cm^2. [25] This indicates a comparable conductivity, considering the difference in thickness. Naturally, the effective cell resistance is not solely a result of the membrane, but also consists of other contributions such as the ionic phase in the electrode or catalyst layer.

While a supporting electrolyte is a necessity for ion-solvating membranes, cells based on AEMs have repeatedly demonstrated increased performance when a supporting electrolyte is introduced or when the concentration is increased[10–14]. Unfortunately, the large majority of

AEMs developed so far are chemically unstable in an alkaline environment and can only operate satisfactorily for a few, to a few hundred, hours[6,11]. The instability is primarily due to the hydroxide ions, which readily react with and degrade the anion exchange groups through nucleophilic displacement and elimination reactions[26]. Another obstacle with the AEMs is their high CO_2 affinity, resulting in the rapid formation of carbonates and bicarbonates and therefore a dramatic conductivity drop when exposed to ambient air[27]. This makes the application of the membranes in their fully hydroxide-exchange form challenging. In this perspective, the presence of KOH(aq) is beneficial, but only so far as the stability of the anion exchange groups or polymer backbone is not critically compromised. In fact, the most impressive polarization behaviour published so far is based on a tetramethyl-imidazolium functionalized styrene AEM operated in 1 M KOH[28].

A key property of membranes or diaphragms is their ability to hinder gas crossover and limit the mixing of evolved hydrogen and oxygen. This may be particularly critical when pressurized cells are operated at part load as the flushing of permeated hydrogen with the produced oxygen is reduced. Crossover is not only important from a safety point of view, but also in terms of efficiency. However, this is often a somewhat neglected aspect. General statements are frequently made, that rightfully address the porous nature of diaphragms as a problem, while proceeding to mention the dense properties of ion exchange membranes as a solution. What is rarely addressed are the differences in dominant crossover mechanisms, which were recently investigated in detail for both alkaline diaphragms and acidic Nafion membranes[29-33]. In short, crossover issues through porous diaphragms primarily stem from convective transport due to differential pressure and the related movement of electrolyte with dissolved gases. For this reason, the rapid ramping of current density can be problematic, as the absolute pressure on each side of the diaphragm must be kept in close proximity. On the contrary, convective crossover is negligible in Nafion-based PEM cells, whereas crossover induced by diffusion through the hydrated microchannel structures of the membrane constitutes a significant effect, with the hydrogen diffusivity in Nafion being more than an order of magnitude larger than in KOH(aq) flooded Zirfon[31]. The diffusive crossover is particularly severe under pressurized operation, as it is proportional to the concentration gradient of dissolved hydrogen, which is in turn proportional to partial pressure, in accordance with Henry's law. Because of this, solubility in the aqueous phase is important, and both hydrogen and oxygen have a larger solubility in pure

water than in aqueous KOH. There is almost an order of magnitude of difference between 0 wt% and 30 wt% aqueous KOH[31,33]. This speaks positively for operating with a concentrated supporting electrolyte and lower hydrogen crossover can be expected from ion-solvating membranes in concentrated KOH(aq) than from PEMs or AEMs with hydrated ionic channels. Low crossover values in the proximity of the resolution limit of the detector were observed. For 80 µm cells operated at 100 and 1000 mA cm^{-2}, the H2-concentrations were in the range of 0.10-0.37%, corresponding to a specific permeability in the vicinity of 3-12 x 10^{-12} mol s^{-1} $cm^{-1}bar^{-1}$. This is about a factor of 5 or more lower than Nafion at 80 °C (a. 5 x 10^{-11} mol s^{-1} $cm^{-1}bar^{-1}$)[30,34] and similar to the Tokuyama A201 AEM at 50 °C (5.6 x 10^{-12} mol s^{-1} $cm^{-1}bar^{-1}$ at 50 °C),[35] and at least indicative of good gas separation properties.

There are other differences at a cell and system level, which change when a supporting electrolyte is employed. For instance, viscosity and surface tension differ from that of pure water, which may in turn affect the bubble dislocation and gas coverage properties of the electrodes. Operating with water or an aqueous electrolyte on only one side of the membrane is perhaps less feasible and balance of plant aspects related to corrosion and catalyst dissolution and re-deposition could be more challenging.

Stability-wise, the use of a supporting electrolyte is not a major challenge when it comes to materials for electrodes, cell hardware and system auxiliary units. The main barrier in the development of this technology is the lack of a chemically-stable and mechanically-robust ion-solvating polymer membrane that can support high ion conductivity. Membranes based on polybenzimidazole indeed exhibit good performance and demonstrate the potential of the cell concept, but are intrinsically unstable in the strongly alkaline environment[18]. Steric protection[36] or enhancement of the electron density[37] around the vulnerable sites are degradation mitigation strategies that have proven particularly successful in this context. A recently published study by Mohanthy *et al.*[39] suggests a correlation between the presence of heteroatoms in the polymer backbone and poor alkali resistance. A rational strategy in alkaline ion-solvating polymer electrolyte membrane development is therefore to shift the focus towards stable backbone chemistries with enhanced electrolyte uptake.

Conclusions

In this paper we present a third and alternative way towards efficient alkaline electrolyte membranes for water electrolysis, by means of ion-solvating membranes. This is in contrast to conventional porous diaphragms or anion exchange membranes, which are conceptually different. Ion-solvating membranes require the presence of an aqueous hydroxide electrolyte similar to conventional systems, but are free of pendant anion exchange groups susceptible to degradation by hydroxide ions in a supporting electrolyte. A key benefit of this concept is the option to omit the ionomer in electrodes, which are commonly a weak point of AEM water electrolyzers. With 24 wt% KOH as the supporting electrolyte and thin polybenzimidazole membranes, we demonstrate polarization behaviour comparable to PEM electrolyzers, without any PGM catalysts or components. The high rate capability of 1700 mA cm^{-2} at 1.8 V at 80°C demonstrates the potential of this concept, with the prospect of combining the polarization performance of PEM electrolyzers with cheap materials associated with alkaline electrolyzers. In a broader perspective, the envisioned electrolyzer system based on abundant raw materials is not only a matter of reduced cost. Equally importantly, and in contrast to the PEM electrolyzer technology, it is scalable beyond the multi GW level since it is not limited by the availability of PGMs, in particular iridium.

Acknowledgements

The authors would like to acknowledge the project Boosting economic electricity storage (BEEST) funded by the EUDP programme in Denmark (no. EUDP17-1: 12542), for its financial contributing.

References

1. Stolten, D. *Hydrogen and Fuel Cells,* Wiley-VCH, Weinheim, 2010).
2. Zeng, K. & Zhang, D. Recent progress in alkaline water electrolysis for hydrogen production and applications, *Prog. Energy Combust. Sci.,* **36,** 307–326 (2010).
3. Carmo, M., Fritz, D. L., Mergel, J. & Stolten, D. A comprehensive review on PEM water electrolysis, *Int. J. Hydrogen Energy,* **38,** 4901–4934 (2013).
4. Babic, U., Suermann, M., Büchi, F. N., Gubler, L. & Schmidt, T. J. Critical Review—Identifying Critical Gaps for Polymer Electrolyte Water Electrolysis Development, *J.*

Electrochem. Soc., **164,** F387–F399 (2017).

5. Rosa, V. M., Santos, M. B. F. & da Silva, E. P. New materials for water electrolysis diaphragms, *Int. J. Hydrogen Energy,* **20,** 697–700 (1995).
6. Varcoe, J. R. *et al.* Anion-exchange membranes in electrochemical energy systems, *Energy Environ. Sci.,* **7,** 3135–3191 (2014).
7. Vermeiren, P., Adriansens, W., Moreels, J. P. & Leysen, R. Evaluation of the Zirfon separator for use in alkaline water electrolysis and Ni-H2 batteries, *Int. J. Hydrogen Energy,* **23,** 321–324 (1998).
8. Schalenbach, M. A Perspective on Low-Temperature Water Electrolysis – Challenges in Alkaline and Acidic Technology, *Int. J. Electrochem. Sci.,* **13,** 1173–1226 (2018).
9. Dekel, D. R. Review of cell performance in anion exchange membrane fuel cells, *J. Power Sources*,**375,** 158–169 (2018).
10. Wu, X. & Scott, K. CuxCo3−xO4 (0 ≤x < 1) nanoparticles for oxygen evolution in high performance alkaline exchange membrane water electrolysers, *J. Mater. Chem.,* **21,** 12344 (2011).
11. Leng, Y. *et al.* Solid-State Water Electrolysis with an Alkaline Membrane, *J. Am. Chem. Soc.,* **134,** 9054–9057 (2012).
12. Pavel, C. C., Cecconi, F., Emiliani, C., Santiccioli, S., Scaffidi, A., Catanorchi, S. and Comotti, M., Highly Efficient Platinum Group Metal Free Based Membrane-Electrode Assembly for Anion Exchange Membrane Water Electrolysis, *Angew. Chemie, Int. Ed.,* **53,** 1378–1381 (2014).
13. Hnát, J., Paidar, M., Schauer, J. & Bouzek, K. Polymer anion-selective membrane for electrolytic water splitting: The impact of a liquid electrolyte composition on the process parameters and long-term stability, *Int. J. Hydrogen Energy,* **39,** 4779–4787 (2014).
14. Gupta, G., Scott, K. & Mamlouk, M. Performance of polyethylene based radiation grafted anion exchange membrane with polystyrene-b-poly (ethylene/butylene)-b-polystyrene based ionomer using NiCo2O4 catalyst for water electrolysis, *J. Power Sources,* **375,** 387–396 (2018).
15. Xing, B. & Savadogo, O. Hydrogen/oxygen polymer electrolyte membrane fuel cells (PEMFCs) based on alkaline-doped polybenzimidazole (PBI), *Electrochem. Commun.,* **2,**

697–702 (2000).

16. Aili, D., Hansen, M.K., Renzaho, R.F., Li, Q., Christensen, E., Jensen, J.O. and Bjerrum, N.J., Heterogeneous anion conducting membranes based on linear and crosslinked KOH doped polybenzimidazole for alkaline water electrolysis, *J. Memb. Sci.,* **447,** 424–432 (2013).
17. Kraglund, M. R. *et al.* Zero-Gap Alkaline Water Electrolysis Using Ion-Solvating Polymer Electrolyte Membranes at Reduced KOH Concentrations, *J. Electrochem. Soc.,* **163,** F3125–F3131 (2016).
18. Aili, D., Jankova, K., Li, Q., Bjerrum, N. J. & Jensen, J. O. The stability of poly(2,2′-(m-phenylene)-5,5′-bibenzimidazole) membranes in aqueous potassium hydroxide, *J. Memb. Sci.,* **492,** 422–429 (2015).
19. Kraglund, M. R. *et al.* Zero-Gap Alkaline Water Electrolysis Using Ion-Solvating Polymer Electrolyte Membranes at Reduced KOH Concentrations, *J. Electrochem. Soc.,* **163,** F3125–F3131 (2016).
20. Henkensmeier, D., Cho, H.-R., Kim, H.J., Nunes Kirchner, C., Leppin, J., Dyck, A., Jang, J.-H., Cho, e., Nam, S.-W., and Lim, T.-H., Polym. Degrad. Stab., **97**, 264-272 (2012)
21. Thomas, O. D., Soo, K. J. W. Y., Peckham, T. J., Kulkarni, M. P. & Holdcroft, *Polym. Chem., 2, 1641* (2011).
22. Schiller, G., Henne, R., Mohr, P. & Peinecke, V. High performance electrodes for an advanced intermittently operated 10-kW alkaline water electrolyzer, *Int. J. Hydrogen Energy,* **23,** 761–765 (1998).
23. Schiller, G. & Borck, V. Vacuum plasma sprayed electrodes for advanced alkaline water electrolysis, *Int. J. Hydrogen Energy,* **17,** 261–273 (1992).
24. Schiller, G., Henne, R. & Borck, V. Vacuum plasma spraying of high-performance electrodes for alkaline water electrolysis, *J. Therm. Spray Technol.,* **4,** 185–194 (1995).
25. Ito, H., Maeda, T., Nakano, A., Kato, A. & Yoshida, T. Influence of pore structural properties of current collectors on the performance of proton exchange membrane electrolyzer, *Electrochim. Acta,* **100,** 242–248 (2013).
26. Marino, M. G. & Kreuer, K. D. Alkaline Stability of Quaternary Ammonium Cations for Alkaline Fuel Cell Membranes and Ionic Liquids, *ChemSusChem,* **8,** 513–523 (2015).
27. Marino, M. G., Melchior, J. P., Wohlfarth, A. & Kreuer, K. D. Hydroxide, halide and

water transport in a model anion exchange membrane, *J. Memb. Sci.,* **464,** 61–71 (2014).

28. Liu, Z., Sajjad, S. D., Gao, Y., Kaczur, J. & Masel, R. I. An Alkaline Water Electrolyzer with Sustainion^{TM} Membranes: 1 A/cm^2 at 1.9V with Base Metal Catalysts, *ECS Trans.,* **77,** 71–73 (2017).
29. Schalenbach, M., Carmo, M., Fritz, D. L., Mergel, J. & Stolten, D. Pressurized PEM water electrolysis: Efficiency and gas crossover, *Int. J. Hydrogen Energy,* **38**, 14921–14933 (2013).
30. Schalenbach, M., Carmo, M., Fritz, D.L., Mergel, J. and Stolten, D., Gas Permeation through Nafion. Part 1: Measurements, *J. Phys. Chem. C,* **119,** 25145–25155 (2015).
31. Schalenbach, M., Tjarks, G., Carmo, M., Lueke, W., Mueller, M. and Stolten, D., *J. Electrochem. Soc.,* **163,** F3197–F3208 (2016).
32. Schalenbach, M., Lueke, W. & Stolten, D. Hydrogen Diffusivity and Electrolyte Permeability of the Zirfon PERL Separator for Alkaline Water Electrolysis, *J. Electrochem. Soc.,* **163,** F1480–F1488 (2016).
33. Trinke., P., Haug, P., Brauns, J., Bensmann, B., Hanke-Rauschenbach, R.,and Turek, T., *J. Electrochem. Soc.,* **165**, F502-F513 (2018)
34. Ito, H., Maeda, T., Nakano, A., Takenaka, H., *Int. J. Hydrogen Energy*, **36**, 10527-10540 (2011)
35. Ito, H., Kawaguchi, N., Someya, S., Munakata, T., Miyazaki, N., Ishida, M., Nakano, A., Int. J. Hydrogen Energy, **43**, 17030-17039 (2018)
36. Thomas, O. D., Soo, K. J. W. Y., Peckham, T. J., Kulkarni, M. P. & Holdcroft, S. A stable hydroxide-conducting polymer, *J. Am. Chem. Soc.,* **134,** 10753–6 (2012).
37. Henkensmeier, D. *et al.* Anion conducting polymers based on ether linked polybenzimidazole (PBI-OO), *Int. J. Hydrogen Energy,* **39,** 2842–2853 (2014).
38. Mohanty, A. D., Tignor, S. E., Krause, J. A., Choe, Y.-K. & Bae, C. Systematic Alkaline Stability Study of Polymer Backbones for Anion Exchange Membrane Applications, *Macromolecules,* **49,** 3361–3372 (2016).
39. Xiao, L., Zhang, S., Pan, J., Yang, C., He, M., Zhuang, L. and Lu, j., *Energy Environ. Sci.,* **5**, 7869 (2012).
40. Cao, Y.-C., Wu, X. & Scott, K. A quaternary ammonium grafted poly vinyl benzyl chloride membrane for alkaline anion exchange membrane water electrolysers with no-

noble-metal catalysts, *Int. J. Hydrogen Energy,* **37,** 9524–9528 (2012).

41. Wu, X. & Scott, K. A polymethacrylate-based quaternary ammonium OH− ionomer binder for non-precious metal alkaline anion exchange membrane water electrolysers, *J. Power Sources,* **214,** 124–129 (2012).
42. Faraj, M., Boccia, M., Miller, H., Martini, F., Borsacchi, S., Geppi, M. and Pucci, A., New LDPE based anion-exchange membranes for alkaline solid polymeric electrolyte water electrolysis, *Int. J. Hydrogen Energy,* **37,** 14992–15002 (2012).
43. Wu, X. & Scott, K. A Li-doped Co3O4 oxygen evolution catalyst for non-precious metal alkaline anion exchange membrane water electrolysers, *Int. J. Hydrogen Energy,* **38,** 3123–3129 (2013).
44. Hnát, J., Plevová, M., Žitka, J., Paidar, M. & Bouzek, K. Anion-selective materials with 1,4-diazabicyclo[2.2.2]octane functional groups for advanced alkaline water electrolysis, *Electrochim. Acta,* **248,** 547–555 (2017).
45. Wu, X., Scott, K., A non-precious metal bifunctional oxygen electrode for alkaline anion exchange membrane cells, *J. Power Sources,* **206,** 14–19 (2012).
46. Parrondo, J., Arges, C.G., Niedzwiecki, M., Anderson, E.B., Ayers, K.E. and Ramani, V., Degradation of anion exchange membranes used for hydrogen production by ultrapure water electrolysis, *RSC Adv.,* **4,** 9875 (2014).
47. Park, E. J., Capuano, C. B., Ayers, K. E. & Bae, C. Chemically durable polymer electrolytes for solid-state alkaline water electrolysis, *J. Power Sources,* **375,** 367–372 (2018).
48. Ahn, S. H., Lee, B.-S., Choi, I., Yoo, S.J., Kim, H.-J., Cho, E., Henkensmeier, D., Nam, S.-W., Kim, S.-K. and Jang, J.H., Development of a membrane electrode assembly for alkaline water electrolysis by direct electrodeposition of nickel on carbon papers, *Appl. Catal. B Environ.,* **154–155,** 197–205 (2014).
49. Schauer, J., Zitka, J., Pientka, Z., Krivcik, J., Hnat, J. and Bouzek, J., Polysulfone-based anion exchange polymers for catalyst binders in alkaline electrolyzers, *J. Appl. Polym. Sci.,* **132,** 42581 (2015).
50. Diaz, L.A., Hnat, J., Heredia, N., Bruno, M.M., Viva, F.A., Paidar, M., Corti, H.R., Bouzek, K. and Abuin, G.C., *J. Power, Sources,* **312**,128-136 (2016)
51. Aili, D. *et al.* Towards a stable ion-solvating polymer electrolyte for advanced alkaline

water electrolysis, *J. Mater. Chem. A,* **5,** 5055–5066 (2017).

52. Chanda, D., Hnát, J., Bystron, T., Paidar, M. & Bouzek, K. Optimization of synthesis of the nickel-cobalt oxide based anode electrocatalyst and of the related membrane-electrode assembly for alkaline water electrolysis, *J. Power Sources,* **347,** 247–258 (2017).

53. Diaz, L. A. *et al.* Alkali-doped polyvinyl alcohol – Polybenzimidazole membranes for alkaline water electrolysis, *J. Memb. Sci.,* **535,** 45–55 (2017).

54. Li, X., Walsh, F. C. & Pletcher, D. Nickel based electrocatalysts for oxygen evolution in high current density, alkaline water electrolysers, *Phys. Chem. Chem. Phys.* **13,** 1162–7 (2011).

Supplementary information

Methods

Membrane preparation. The *m*-PBI polymer (inherent viscosity 1.9 dL g^{-1} measured at 30.0°C in an Ubbelohde viscometer, 96% H_2SO_4 with 500 mg dL^{-1} solid content) was synthesized in-house according to common procedures, as described elsewhere[50]. The polymer was cast from a DMAc solution (4.6% solid content) in petri dishes to form membranes of dry thicknesses of 20 and 40 µm. After careful washing in demineralized water at 90°C for at least 4 h, the membranes were doped at room temperature at least overnight prior to cell assembly by submersion in 24 wt% KOH (aq), resulting in approximately a doubling of thickness due to swelling, yielding membrane thicknesses of approximately 40 and 80 µm. Zirfon PERL (500 µm) was supplied by Agfa.

Electrode preparation. Perforated nickel plates were supplied by Veco B.V. with a thickness of 340 µm, a void fraction of 60% and a hole diameter of 1.2 mm. Uncoated perforated plate electrodes were welded to the nickel flowfield plates when used as anodes. The Raney nickel electrodes used in this study were fabricated at German Aerospace Center (DLR), Stuttgart, Germany by means of vacuum plasma spraying (VPS). The procedure has been described in detail in previous publications[37–39]. For the cathode coatings (hydrogen evolution) gas-atomized Ni-Al-Mo alloy powder containing 39 wt% Ni, 44 wt% Al, and 17 wt% Mo (H.C. Starck, Germany) with a particle size below 40 µm was used. The anode coatings were prepared from a Ni-Al alloy powder composed of 56 wt% Ni and 44 wt% Al. The powders were plasma sprayed onto 340 µm thick perforated Ni sheets. The thermal spray parameters were: 25 kW torch power (430 A, 57 V), 45 SLPM (standard liters per minute) Ar, 4 SLPM H_2 and 10 SLPM He as plasma gases, 70 mbar tank pressure and 200 mm spraying distance. Prior to coating, the Ni sheets were grit-blasted and chemically etched using a 34% HCl solution. The layer thickness was in the range of 110-130 µm. Activation of the Raney Ni electrodes was performed in 24 wt% KOH with 100 g L^{-1} sodium-tartrate dihydrate to complex the leached out aluminium hydroxides and prevent precipitation of aluminium hydroxides. About 50-100 cm^2 (2-4 electrodes) were activated per half-liter of solution. The solution was heated to 80°C, and the electrodes were

submerged for 24 hours, after which they were removed, rinsed and stored in water to prevent pyrophoric re-oxidation.

Cell test and electrochemical characterization. Square-shaped 5 cm × 5 cm electrodes were assembled horizontally with the separators in a zero gap configuration using Ni bipolar plates and polytetrafluoroethylene (PTFE) gaskets. The flowfield design was a pin-type. The cells were operated vertically and 24 wt% KOH electrolyte was circulated in two partially separated circuits with 50 ml min^{-1} by PTFE diaphragm pumps. The KOH (aq) was prepared from KOH pellets (assay >85%) and MiliQ water, but was otherwise used as-prepared without any purification. Two 1.5 L storage tanks were connected by a narrow tube in the bottom to equilibrate the electrolyte levels. Heating was performed in a pre-heating cell, as well as in the test cell, and the temperature was increased to 80°C prior to starting the cell.

A typical cell test was initiated by a 12 hour break-in at 40 mA cm^{-2} followed by a step-wise galvanostatically-recorded polarization curve with 5 minutes per current density point, up to either a limit of 2.8 V or 4 A cm^{-2}. Galvanostatic electrochemical impedance spectroscopy (GEIS) was recorded at several current steps in a separate polarization curve immediately following the primary polarization curve. The impedance response was recorded in the frequency range of 25 kHz-1 Hz with an amplitude corresponding to 10% of the current density setpoint. The cells were kept for 1-2 minutes at each current density step prior to recording the impedance measurements. The electrochemical data were recorded with a Biologic HCP 1005 potentiostat. For the long-term tests a Conradi Electronic GmbH power supply was used and manually set, alternatingly, to 100 or 1000 mA cm^{-2}, while the cell potential was monitored with a Biologic HCP1001 potentiostat. Water was regularly supplied by hand to keep the electrolyte concentration constant. For long-term tests, the anode gas was passed through a bubble flask and drying steps with silica gel and molecular sieves, after which the H_2 in O_2 level was monitored with a flame ionization detector (FID). Gas was occasionally sampled for gas chromatography analysis, which revealed good correspondence with the FID values.